The effect of oxygen isotope substitution on magnetic properties of $(La_{1-y}Pr_y)_{0.7}Ca_{0.3}MnO_3$ manganites

1999 J. Phys.: Condens. Matter 11 5865

(http://iopscience.iop.org/0953-8984/11/30/315)

J. Phys.: Condens. Matter **11** (1999) 5865–5873. Printed in the UK PII: S0953-8984(99)03947-8

The effect of oxygen isotope substitution on magnetic properties of $(La_{1-y}Pr_y)_{0.7}Ca_{0.3}MnO_3$ manganites

N A Babushkina†, L M Belova†, A N Taldenkov†, E A Chistotina†, D I Khomskii‡§, K I Kugel‖, O Yu Gorbenko¶ and A R Kaul¶

† 'Kurchatov Institute' Russian Research Centre, 1 Kurchatov Square, Moscow, 123182, Russia
‡ Materials Science Centre, University of Groningen, Nijenborgh 4, 9747 AG Groningen, The Netherlands
§ Lebedev Physics Institute, Leninskii Prospekt 53, Moscow, 117924, Russia
‖ Scientific Centre for Applied Problems in Electrodynamics, 13/19 Izhorskaya Street, Moscow, 127412, Russia
¶ Chemistry Department, Moscow State University, Vorobievy Gory, Moscow, 119899, Russia

Received 5 May 1999

Abstract. The effect of oxygen isotope substitution on the alternating-current magnetic susceptibility for $(La_{1-y}Pr_y)_{0.7}Ca_{0.3}MnO_3$ ceramics ($y = 0$, 0.25, 0.5, 0.75, 1) was studied in the temperature range 4.2–300 K. At $y < 0.75$, the low-temperature behaviour of these manganites is typical for a ferromagnetic metal, whereas at y close to 1, the system behaves as an antiferromagnetic charge-ordered insulator. The $^{16}O \rightarrow {}^{18}O$ isotope substitution significantly shifts the Curie point T_C, but has a smaller effect on the Néel temperature T_N. At the crossover concentration $y = 0.75$, the exchange of ^{16}O with ^{18}O gives rise to a metal–insulator transition. The temperature dependence of the magnetic susceptibility is characterized by a pronounced hysteresis at $y \neq 0$ or 1, and the width of the hysteresis loops is strongly affected by the $^{16}O \rightarrow {}^{18}O$ exchange. The behaviour of the susceptibility in the paramagnetic phase gives an indication of the phase separation over quite a wide temperature range near the transition point. The phase diagram in the T–y plane is obtained and its modification with isotope substitution is discussed.

1. Introduction

Mixed lanthanum–praseodymium manganites with the $(La_{1-y}Pr_y)_{0.7}Ca_{0.3}MnO_3$ composition exhibit a variety of electrical and magnetic properties ranging from those of ferromagnetic metal at $y = 0$ to those of an antiferromagnetic charge-ordered insulator at $y = 1$ [1]. The most interesting effects caused by an interplay of different types of ordering should be expected at concentrations y corresponding to the crossover between these two regimes. In the crossover region, the strong coupling between lattice, spin and charge degrees of freedom gives rise to some unusual features of this system and, in particular, to the anomalously large isotope effect. Earlier [2, 3], we studied the effect of oxygen isotope substitution on the electrical resistivity of these manganites. For ceramic samples with $y = 0.75$, it was found that $^{16}O \rightarrow {}^{18}O$ substitution results in a reversible metal–insulator transition: the sample annealed in ^{16}O had a metal-like conductivity below $T_C = 95$ K and the sample annealed in ^{18}O behaved as an insulator in zero magnetic field. The isotope-driven metal–insulator transition was also observed in $(La_{0.5}Nd_{0.5})_{0.7}Ca_{0.3}MnO_3$ [4]. Such a unique sensitivity of the system to the oxygen isotope substitution gives a clear indication of the important role of electron–phonon interaction in the transport properties of perovskite manganites. The results were

0953-8984/99/305865+09$30.00

discussed in terms of the dependence of the hopping integral on the isotope composition in the vicinity of the charge-ordering transition giving rise to the insulating state [3]. Neutron powder diffraction studies [5] of the samples with $y = 0.75$ demonstrated that $^{16}O \rightarrow {}^{18}O$ substitution suppressed the ferromagnetism and stabilized the antiferromagnetism accompanied by charge ordering.

It is of interest to study the isotope effect in $(La_{1-y}Pr_y)_{0.7}Ca_{0.3}MnO_3$ at different values of y, i.e. with the variation of the average radius $\langle r \rangle$ of the rare-earth ion. The temperature dependence of the electrical resistivity $\rho(T)$ for this system was reported in reference [1]. The temperature of the resistivity peak corresponding to the Curie point T_C decreases with the increase of y, and at $y > 0.75$ the system appears to be insulating. It was mentioned above that such a crossover is accompanied by a magnetic transition: the ferromagnetic (FM) ordering in the metal-like phase is changed to antiferromagnetic (AF) ordering coexisting with charge ordering (CO) in the insulating phase. Thus, the metal–insulator transition induced by the oxygen isotope exchange takes place in the vicinity of the FM–AF boundary in the phase diagram. At this concentration, the system turns out to be very sensitive to any parameter shifting the FM–AF equilibrium.

In this paper, we analyse the evolution of the magnetic phase diagram of the $(La_{1-y}Pr_y)_{0.7}Ca_{0.3}MnO_3$ system with variation of the Pr content and its changes induced by $^{16}O \rightarrow {}^{18}O$ substitution. The Ca content and hence the Mn^{3+}/Mn^{4+} ratio (hole doping level) remained unchanged. Our analysis is based on measurements of the ac magnetic susceptibility and electrical resistivity at $y = 0$, 0.25, 0.5, 0.75, and 1. We also used the reported data on the effect of $^{16}O \rightarrow {}^{18}O$ exchange on the magnetic structure of at $y = 0$ [6] and $y = 0.75$ [5].

2. Experimental procedure

The samples were prepared by the so-called 'paper route': ash-free paper filters were soaked in aqueous solutions of La, Pr, Mn, and Ca nitrates present in the necessary proportions. The dried (at 120 °C) filters were burned and the resulting powder was calcined in air at 700 °C for 2 h. Then the powder was pressed into pellets and sintered in air at 1200 °C for 12 h. For the susceptibility measurements, the pellets were ground to powder. The x-ray diffraction analysis verified the phase homogeneity of all of the compositions and demonstrated that the samples had the orthorhombic crystal structure.

The isotope enrichment of the $(La_{1-y}Pr_y)_{0.7}Ca_{0.3}MnO_3$ samples was performed at $T = 950$ °C at the oxygen pressure $p = 1$ atm. Pairs of samples with the same compositions were annealed simultaneously, one sample in the ^{16}O atmosphere (with 99.7% enrichment) and the other in the ^{18}O atmosphere (with 85% enrichment). The powders, in platinum crucibles, were placed in separate quartz tubes mounted in the furnace parallel to each other. Each tube formed part of a closed loop with the circulating ^{16}O and ^{18}O, respectively. The samples were annealed in oxygen for 48 h at 950 °C and were slowly cooled down to room temperature. The ^{18}O content in the samples produced was equal to 80% as determined by the weight changes after the isotope enrichment. The $y = 0.75$ composition was tested for oxygen stoichiometry by the methods of neutron powder diffraction and iodometric titration [5]. The difference obtained between the oxygen contents of the samples annealed in ^{16}O and annealed in ^{18}O was less than 0.002.

The electrical resistivity was measured by the conventional four-probe technique at temperatures ranging from 4.2 to 300 K. The measurements of the ac magnetic susceptibility $\chi_{ac}(T)$ were performed in an ac magnetic field with frequency 667 Hz and amplitude about 0.1 Oe.

3. Results

To characterize the transport properties of the system under discussion, we measured the temperature dependence of the electrical resistivity of the initial $(La_{1-y}Pr_y)_{0.7}Ca_{0.3}MnO_3$ samples with $y = 0$, 0.25, 0.5, 0.75, and 1 before their annealing in oxygen. The corresponding curves are presented in figure 1. The electrical resistivity $\rho(T)$ steeply decreases below T_C. With the growth of y (i.e., with the increase in Pr content corresponding to the decreasing $\langle r \rangle$) T_C decreases from 260 K at $y = 0$ to 95 K at $y = 0.75$. These results agree with those reported in reference [1].

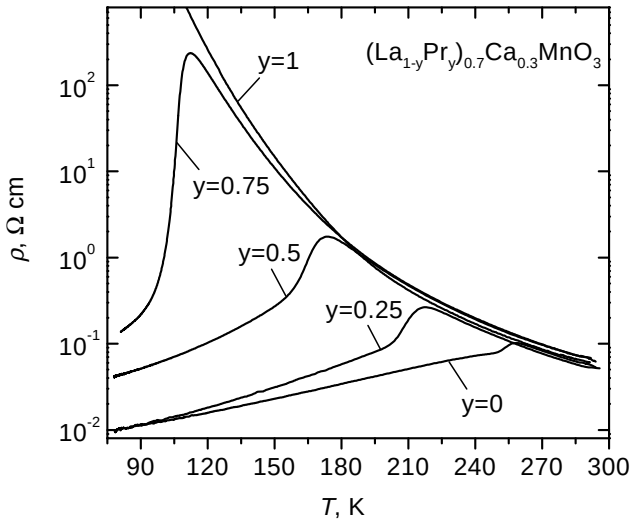

Figure 1. Temperature dependences of the electrical resistivity of the $(La_{1-y}Pr_y)_{0.7}Ca_{0.3}MnO_3$ ceramics for various Pr concentrations. Resistivity measurements were made on the 'as-grown' materials prior to any annealing in oxygen.

The magnetic properties were studied by measuring the ac magnetic susceptibility $\chi_{ac}(T) = \chi' + i\chi''$. The $\chi'(T)$ curves for the powder samples of all compositions studied, annealed in ^{16}O or in ^{18}O, are presented in figure 2. For each sample, we plotted the $\chi'(T)$ curves measured on cooling and on heating to demonstrate the thermal hysteresis.

Let us first consider $\chi'(T)$ for the ^{16}O-annealed samples. We can see the same tendency as for the $\rho(T)$ data—that is, the decrease of the ferromagnetic transition temperature T_C with the increase of y. The Curie temperature T_C determined from the maximum of the derivative $|d\chi'/dT|$ decreases from 260 K to 95 K with increase of y from zero to 0.75. At $y = 1$, the susceptibility curve has the form characteristic of AF ordering.

Note that only at $y = 0$ and 0.25 are the $\chi'(T)$ curves typical for the pure ferromagnetic material; the temperature dependences of χ' for $y = 0.5$ and 0.75 are more complicated. In the latter case, we observe a pronounced thermal hysteresis: the cooling curve is shifted towards lower temperatures and the transition from the paramagnetic (PM) to the FM state is more smeared than on heating. On heating, the low-temperature metallic state is apparently quenched, and this causes the shift of the heating curve to higher T. The width of the hysteresis loop is largest for the sample with $y = 0.75$ (about 35 K).

The hysteretic behaviour implies that the PM–FM transition is of first order for these

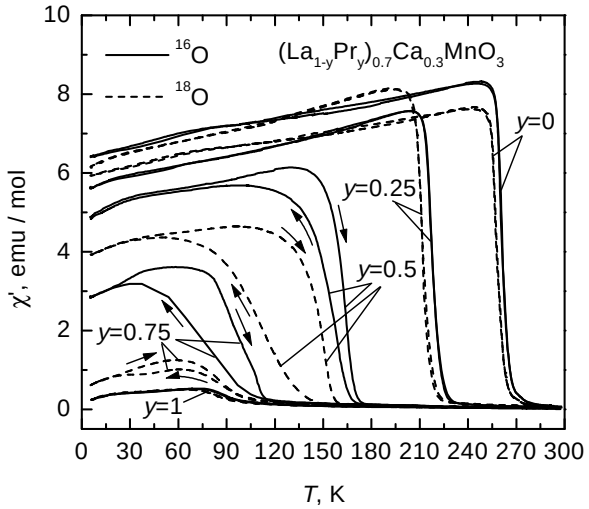

Figure 2. The real part of the ac magnetic susceptibility versus temperature for the $(La_{1-y}Pr_y)_{0.7}Ca_{0.3}MnO_3$ samples annealed in ^{16}O and ^{18}O for various Pr concentrations. Arrows indicate heating and cooling.

samples. This can be related to the coexistence of FM and AF states. Such a coexistence was observed by means of neutron powder diffraction [5] for the sample with $y = 0.75$ annealed in ^{16}O. The neutron data show that the onset of FM ordering occurs at $T_C = 120$ K, and the magnetization attains saturation at 80 K. The AF phase appears at $T_N = 150$ K and the corresponding sublattice magnetization reaches its maximum at $T = 110$ K, correlating with the onset of FM ordering. At lower temperatures, the AF sublattice magnetization steeply decreases and nearly vanishes at 80 K. This seems to be related to the inhomogeneous state corresponding to the phase separation at temperatures below the onset of ferromagnetism. The form of the $\chi'(T)$ curve at $y = 0.75$ corresponds to this picture: the tendency towards phase separation manifests itself in the large width of the hysteresis loop. The samples with $y < 0.75$ are not so close to the FM–AF phase boundary; hence the phase separation is not so pronounced, and the hysteresis loops become narrower. At $y = 1$, we have $\chi'(T)$ typical of AF ordering with a peak near T_N.

For the samples annealed in the ^{18}O atmosphere, $\chi'(T)$ has similar characteristic features, but all curves and the values of the transition points are shifted towards the lower temperatures. For samples with $y = 0$ and 0.25, where only ferromagnetic ordering exists, the Curie temperature T_C for ^{18}O samples decreases by 6 K and 10 K, respectively. The sample with $y = 0.5$ exhibits behaviour characteristic of the inhomogeneous state, similar to that observed for the ^{16}O sample, but the contribution of AF ordering seems to increase for the ^{18}O sample, and hence the $\chi'(T)$ hysteresis loop is wider in this case. This is an indication that the ^{18}O sample with $y = 0.5$ is near the FM–AF phase boundary and exhibits an enhanced tendency towards phase separation. For the sample with $y = 0.75$ annealed in ^{18}O, the FM state disappears, as follows from the neutron diffraction data [5], and only antiferromagnetic ordering survives. Therefore in figure 2, we see a peak in the $\chi'(T)$ curve for this sample similar to that observed at $y = 1$ for the sample annealed in ^{16}O. The $^{16}O \rightarrow {}^{18}O$ isotope substitution for the sample with $y = 1$ did not produce any appreciable effect on the form of the $\chi'(T)$ curve. Thus, the form of hysteresis depends both on y and on the oxygen isotope substitution, and the hysteresis

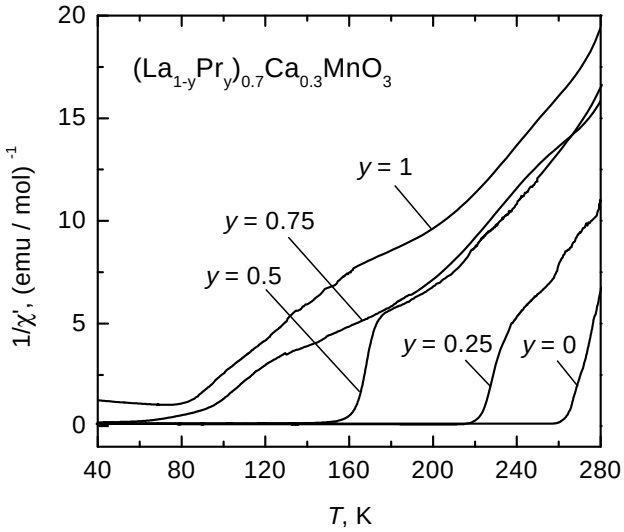

Figure 3. Inverse susceptibility versus temperature for the $(La_{1-y}Pr_y)_{0.7}Ca_{0.3}MnO_3$ samples annealed in ^{16}O for various Pr concentrations, measured on cooling.

loops have maximum width for the samples with compositions in the vicinity of the FM–AF phase boundary ($y = 0.75$ and 0.5 for the samples annealed in ^{16}O and ^{18}O, respectively).

The temperature dependence of the inverse susceptibility $1/\chi'(T)$ measured on cooling is shown in figure 3 for all of the samples ($y = 0$–1) annealed in ^{16}O. It is important to note that in the paramagnetic state we do not observe any sizable isotope effect in the magnetic susceptibility. At $y \neq 0$ or 1, the steepest part of the $1/\chi'(T)$ curves is in the vicinity of the magnetic transition. This large slope corresponds to the hysteretic (phase-separated) region in the $\chi'(T)$ dependence. Then, the growth of $1/\chi'$ with temperature becomes slower, and the linear extrapolation of this portion leads to the intersection of the corresponding line with the T-axis at temperatures much lower than T_C. At higher temperatures, the slope becomes larger again ($y = 0.75$ and 0.5), and the lines extrapolating this portion intersect the T-axis at $T > T_C$. This behaviour suggests the existence of certain antiferromagnetic spin correlations above T_C.

In the next section, we discuss the mechanisms that may be responsible for the unusual behaviour of the inverse susceptibility.

4. Discussion

We see that the increase in the praseodymium content (up to $y = 0.75$) results in a more clearly pronounced thermal hysteresis, which is a general signature of the first-order phase transitions and of the phase separation accompanying them. The existence of a magnetic first-order transition usually gives an indication of the coupling of the spin subsystem with lattice distortions, inhomogeneous electron-density distribution, or with some other types of ordering. The Pr-based manganites exhibit, in general, a tendency towards charge ordering, i.e., towards a regular arrangement of Mn^{3+} and Mn^{4+} ions, which is revealed by the distortions of oxygen octahedra around Mn^{3+}. Interplay of the magnetic and charge ordering (or, within a more general approach, between the spin, electron, and lattice subsystems) should favour the

thermal hysteresis, and the width of hysteresis loops indirectly characterizes the strength of the corresponding coupling. The maximum hysteresis width is observed, as should be expected, for the samples with $y = 0.5$ and 0.75 having compositions close to the phase boundary between FM and AF states. It was already mentioned in the introduction that just in the vicinity of this boundary there occurs a transformation not only of the spin structure, but also of the electron and lattice structures as well. This signifies here the tight interrelation between these three systems. The coexistence of different order parameters is clearly illustrated by the neutron diffraction studies of the powder samples with $y = 0.75$. In both ^{16}O and ^{18}O samples, a superstructure related to the charge ordering was observed below $T_{CO} = 170$ K [5]. However, in the sample annealed in ^{16}O the intensity of the corresponding peaks decreases with temperature simultaneously with growth of the FM order, whereas in the sample annealed in ^{18}O, where the ferromagnetic component is absent, the intensity of the CO peaks reaches saturation.

Clear indications of the coupling between the spin and electron systems are given by the temperature dependence of the inverse susceptibility $1/\chi'(T)$. The $1/\chi'(T)$ curves for the samples with $y = 0.5$ and 0.75 exhibit a variable slope in the paramagnetic region. Thus, in different temperature regions $\chi'(T)$ exhibits behaviour similar to the Curie–Weiss law $\chi'(T) \propto 1/(T - \Theta_C)$ with different Θ_C values. It is well known that Θ_C is determined by the exchange integral of the spins of magnetic ions. For manganites, the exchange integral is directly related to the charge-carrier density (according to the double-exchange mechanism). If the electron density is non-uniformly distributed close to the Curie temperature (there are ferromagnetic droplets, magnetic polarons, etc), then Θ_C is determined by the combination of the regions with locally higher charge density c_{loc} with ferromagnetic spin correlations and by the remaining charge-depleted part with dominant antiferromagnetic correlations, rather than simply by the average charge density $\langle c \rangle$. At higher temperatures, the system appears to be outside the stability range of inhomogeneities, and Θ_C becomes proportional to $\langle c \rangle$. The temperature dependence of the local spin correlations can result in changes in the magnitude or even in the sign of the effective Θ_C. The related problem concerning the possibility of two different Θ_C values was discussed in reference [7]. Different slopes of the inverse susceptibility curves in the paramagnetic region were also observed for La-based manganites [8, 9].

The eventual spin correlations corresponding to $\langle c \rangle$ can develop through a sequence of more or less stable intermediate states. These changes in the spin–spin correlations can cause the stepwise behaviour of the $1/\chi'(T)$ curves. Such steps of $1/\chi'(T)$ were reported in reference [9] for $La_{0.7}Ca_{0.3}MnO_3$ samples. However, for our system, the picture can be even more complicated because of the possible temperature-induced crossover between the ferromagnetic and antiferromagnetic spin correlations. This mechanism responsible for the variable slope in our case results in quite a broad plateau in $1/\chi'(T)$ being observed for the $La_{0.25}Nd_{0.25}Ca_{0.5}MnO_3$ system, exhibiting the AF–FM transition with the temperature decrease [10]. For the system under study, the apparent changes in the spin correlations seem to be related to the vicinity of the FM–AF phase boundary.

On the basis of the data on the temperature dependence of the magnetic susceptibility, we can draw a schematic phase diagram in the T–y plane; this is presented in figure 4. The lines connecting experimental points correspond to the transition between the paramagnetic and the magnetically ordered states (FM or AF) in the samples annealed in ^{16}O and ^{18}O. The distance between the upper and lower curves is equal to the width of the hysteresis loops (hatched regions). We can see that both shaded regions are broadest for those values of concentration y that correspond to the crossover between the FM and AF regimes. This crossover is also accompanied by the formation of charge ordering [5]. Therefore, at these concentrations we have the most pronounced effects related to the spin–lattice coupling and the tendency towards

formation of an inhomogeneous state. For the samples annealed in ^{18}O, the crossover region is shifted towards the lower y-values as compared to the case for the samples annealed in ^{16}O (from $y = 0.75$ for ^{16}O to $y = 0.5$ for ^{18}O). In the region between $y = 0.75$ and 0.5 the $^{16}\text{O} \rightarrow {}^{18}\text{O}$ isotope substitution is expected to give rise to the FM–AF transition and to the metal–insulator transition accompanying it. We mentioned above that such a dramatic change in the temperature dependence of the resistivity accompanying the oxygen isotope substitution was observed earlier for ceramics with $y = 0.75$ [2, 3]. The possible phases and phase boundaries based on the magnetic and neutron data are schematically drawn in the inset to figure 4.

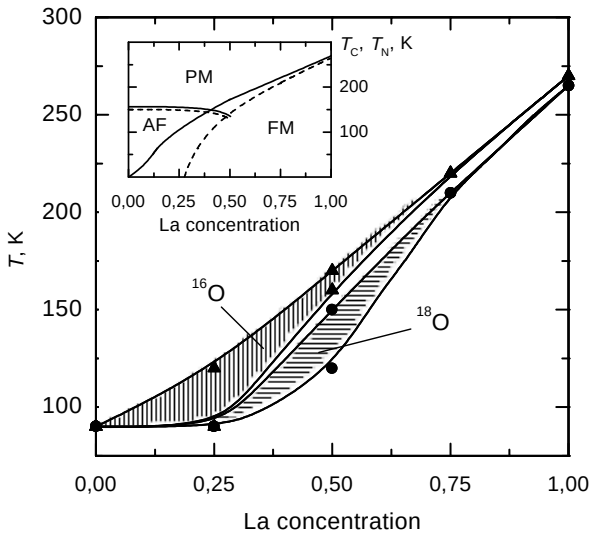

Figure 4. The phase diagram constructed from the different temperatures characterizing magnetic transitions in the $\chi'(T)$ curves for the $(La_{1-y}Pr_y)_{0.7}Ca_{0.3}MnO_3$ system. Triangles and circles correspond to the samples annealed in ^{16}O and ^{18}O, respectively. Hatched regions illustrate the hysteretic regime. Inset: the hypothetical phase diagram based on magnetic and neutron data. FM, AF, and PM denote ferromagnetic, antiferromagnetic, and paramagnetic states, respectively.

Note that the isotope shift of the phase transition points in the ferromagnetic region is much more pronounced than in the antiferromagnetic one. In other words, the isotope effect for the Néel temperature T_N is smaller than for the Curie point T_C. This seems to stem from the difference between the mechanisms responsible for the ferromagnetism (double exchange) and antiferromagnetism (superexchange). In the case of double exchange, we have $T_C \propto t_{\text{eff}}$, where t_{eff} is the effective electron hopping integral renormalized due to the electron–phonon interaction (polaronic band narrowing), whereas $T_N \propto t^2/U$ (U is the on-site Coulomb repulsion), where t is almost non-renormalized [11].

In fact, according the simplest polaron picture, the effective electron or hole hopping matrix element is renormalized as

$$t \rightarrow t_{\text{eff}} = t \exp(-E_{\text{pol}}/\omega). \tag{1}$$

One can write down $E_{\text{pol}} \propto g^2/\omega$, where g is an electron–phonon coupling constant (dimensional) in the Fröhlich Hamiltonian. Here, everywhere, ω is a typical phonon frequency of the order of ω_{Debye}. The dimensionless electron–phonon coupling constant (the one which enters, for example, in superconductivity) is $\lambda \approx g^2 N(0)/\omega$, and it is well known that it does

not depend on the ionic mass. Thus, $1/\omega$ remains in the exponent in equation (1), i.e., the polaronic band narrowing depends on the ionic mass:

$$t_{\text{eff}} \propto t \exp(-\text{constant} \times \sqrt{M}). \tag{2}$$

In the double-exchange model, $T_C \propto t_{\text{eff}}$, i.e. one should expect a rather strong change of T_C with M. On the other hand, for the antiferromagnetic ordering in the insulating state, T_N is given crudely by an expression like

$$T_N \propto J \approx t^2/U \tag{3}$$

where U is the on-site Coulomb (Hubbard) repulsion.

Now, the question arises of what t we should use in equation (3): the bare one or the renormalized t_{eff}-value. One can show (see reference [11]) that in typical cases, the electron–phonon coupling (i.e. the polaronic effect) does not renormalize the superexchange J (in the presence of orbital degeneracy, some renormalization of J can still occur [11]). This has a very simple physical meaning: virtual hoppings of localized electrons to neighbouring sites leading to the superexchange (see equation (3)) are very fast (a typical timescale is $\sim\hbar/U$) and the lattice has no time for relaxation, so the polaronic states are not formed during this process.

Let us also note the difference between the Néel temperature T_N and the charge ordering temperature T_{CO}. In the simple model, the latter is determined by the parameter t_{eff}/V (V is the intersite Coulomb repulsion of electrons) [3, 12]. Thus T_{CO} can be more isotope dependent than T_N. A large isotope shift of T_{CO} was recently reported for La- and Nd-based manganites [13, 14].

5. Conclusions

We demonstrated that oxygen isotope substitution causes substantial changes in the temperature dependence of the magnetic susceptibility for La–Pr manganites with different values of the La/Pr ratio. The data clearly suggest the existence of an inhomogeneous state, especially in the vicinity of the ferromagnetic–antiferromagnetic phase boundary in the magnetic phase diagram. The isotope effect, dramatically enhanced in this system, is a manifestation of a strong interplay between spin, charge, and lattice degrees of freedom, especially at the crossover between the ferromagnetic and antiferromagnetic regions. This interplay favours the formation of an inhomogeneous state, and even provides the changes in the spin–spin interaction in the paramagnetic region.

Acknowledgments

We are grateful to A V Inyushkin and A S Lagutin for helpful assistance. The work was supported by INTAS (project INTAS-97-0963), the INTAS-RFBR program (project IR-97-1954), and RFBR (projects 96-15-96738 and 96-15-97248). The work of DIKh was supported by the Netherlands Foundation for Fundamental Research (FOM) and by the European network OXSEN.

References

[1] Hwang H Y, Cheong S-W, Radaelli P G, Marezio M and Batlogg B 1996 *Phys. Rev. Lett.* **75** 914
[2] Babushkina N A, Belova L M, Gorbenko O Yu, Kaul A R, Bosak A A, Ozhogin V I and Kugel K I 1998 *Nature* **391** 159

[3] Babushkina N A, Belova L M, Ozhogin V I, Gorbenko O Yu, Kaul A R, Bosak A A, Khomskii D I and Kugel K I 1998 *J. Appl. Phys.* **83** 7369
[4] Zhao G-M, Keller H, Hofer J, Shengelaya A and Müller K A 1997 *Solid State Commun.* **104** 57
[5] Balagurov A M, Pomyakushin V Yu, Sheptyakov D V, Aksenov V L, Babushkina N A, Belova L M, Taldenkov A N, Inyushkin A V, Fisher P, Gutmann M, Keller L, Gorbenko O Yu, Amelichev V A and Kaul A R 1999 *Pis. Zh. Eksp. Teor. Fiz.* **69** 46 (Engl. transl. 1999 *JETP Lett.* **69** 50)
[6] Zhao G-M, Conder K, Keller H and Muller K A 1996 *Nature* **381** 676
[7] Nagaev E L and Podel'shchikov A I 1987 *Fiz. Tverd. Tela* **29** 3375 (Engl. transl. 1987 *Sov. Phys.–Solid State* **29** 1935)
[8] Anil Kumar P S, Joy P. A and Date S K 1998 *J. Phys.: Condens. Matter* **10** L269
[9] Amaral V S, Araujo J P, Pogorelov Yu G, Soussa J B, Tavares P B, Vieira J M, Lopes dos Santos J M B, Lourenco A A C S and Algarabel P A 1998 *J. Appl. Phys.* **83** 7154
[10] Arulraj A, Biswas A, Raychaudhuri A K, Rao C N R, Woodward P M, Vogt T, Cox D E and Cheetham A K 1998 *Phys. Rev.* B **57** R8115
[11] Kugel K I and Khomskii D I 1980 *Zh. Eksp. Teor. Fiz.* **79** 987 (Engl. transl. 1980 *Sov. Phys.–JETP* **52** 501)
[12] Khomskii D I 1969 *Preprint* 105 (Lebedev Physics Institute, Moscow)
[13] Zhao G-M, Ghosh K, Keller H and Greene R L 1999 *Phys. Rev.* B **59** 81
[14] Zhao G-M, Ghosh K and Greene R L 1998 *J. Phys.: Condens. Matter* **10** L737